We are IntechOpen, the world's leading publisher of Open Access books Built by scientists, for scientists

4,800
Open access books available

122,000
International authors and editors

135M
Downloads

Our authors are among the

154
Countries delivered to

TOP 1%
most cited scientists

12.2%
Contributors from top 500 universities

CLARIVATE ANALYTICS
BOOK CITATION INDEX
INDEXED

WEB OF SCIENCE™

Selection of our books indexed in the Book Citation Index
in Web of Science™ Core Collection (BKCI)

Interested in publishing with us?
Contact book.department@intechopen.com

Numbers displayed above are based on latest data collected.
For more information visit www.intechopen.com

Application of Morphometric and Stereological Techniques on Analysis and Modelling of the Avian Lung

John N. Maina

'I often say that when you can measure what you are speaking about, and express it in numbers, you know something about it; but when you cannot express it in numbers, your knowledge is of a meager and unsatisfactory kind; it may be the beginning of knowledge, but you have scarcely, in your thoughts, advanced to the stage of science, whatever the matter may be'.

Lecture 'Electrical Units of Measurement' (3 May 1883)

William Thompson (Lord Kelvin) (1824–1907).

Abstract

For a long time, biology was a qualitative (descriptive) science. The investigations failed to fully explicate the functional designs of whole organisms and their constituent parts. About half a century ago, at an interdisciplinary meeting which was held in Feldberg (Germany), the International Society of Stereology (ISS) was formed. Mathematicians, statisticians and physical and biological scientists combined their skills to create a new scientific discipline of stereology that allowed for reliable and reproducible quantitation of structural entities of composite physical and biological materials and extrapolation of measurements made on two-dimensional profiles/images to their three-dimensional forms. With time, novel bias-free sampling and quantitation techniques have been developed and tested. Presently, there is no justification for totally descriptive biological studies. Numerous books, publications, computer programmes and applications and dedicated microscopes exist for cost-effective analysis. Within the relatively short time, it has been in existence, the ISS has actively advanced stereology which is now applied by scientists all over the world in various biological disciplines. Only basic understanding of mathematics, geometry and statistics is needed to do good stereology. Here, analysis of the avian (bird) lung is given to show the versatility and robustness of stereological techniques in analysing biological structures.

Keywords: stereology, morphometry, sampling, avian lung

1. Introduction

In biological studies, by default or design, the primary objective is to understand the relationships between the structure and the function of an organism or animal. The nature and organization of the cellular and tissue constituent parts specify its form and performance. For a long time, in rigidly compartmentalized scientific disciplines, it was not possible to correlate these aspects mainly because disciplines such as physiology and biochemistry generated functional (i.e. quantitative) data, structural studies such as morphology and anatomy were fundamentally descriptive. During the last half century, however, methods that allow biological structures to be meaningfully analysed have been developed by essentially synthesizing statistical and mathematical methods. Biology has profoundly changed from a mere observational, descriptive and classificatory discipline into a fully fledged branch of science with complex theories and concepts of quantitation and formulation of comprehensive mathematical models that powerfully explicate the forms and functions of complex dynamic systems. Quantifying and comparing different biological systems that share common design principles powerfully explain evolutionary and adaptive changes [1].

Quantitative studies require careful planning and execution. Before performing such a study, thorough understanding of the structure of a biological entity and its formative parts is imperative. A pilot study should precede the study and proper research questions formulated from it. A well-planned and properly executed quantitative study must adequately support or refute articulated research questions: *data should not be acquired for their own sake.*

The tissues analysed must be handled and processed carefully. This is to avoid introduction of artefacts during stages like sampling, processing, fixing and staining. The primary goal should be that the tissue analysed is preserved in its initial (natural) state. Since only a small fraction of the organ or tissue can routinely be analysed (**Figure 1**), rigorous unbiased and reproducible sampling is critical to meaningful quantitative studies [2, 3].

Morphometry means measurement of form (**morph** = form and **metric** = measurement), while stereology, which translates from its Greek roots 'stereo' and 'logos', means the 'science of studying solids'. Specifically, it entails extrapolation of measurements made on two-dimensional (2D) profiles/images to their three-dimensional (3D) configuration. In stereological studies, this entails reconstruction of the structural profiles to their in-life state. However, stereology is morphometry, but morphometry is not necessarily stereology.

A tailor who takes measurements of a person in order to make him or her a suit performs morphometry and not stereology. In the use of the highly informative transmission microscopes, be it light or electron, thin sections of tissues have to be cut to allow light or electron beam to pass through. The inescapable action converts 3D structures to 2D profiles (**Figure 2**). The profiles that are generated after sectioning cells, tissues or organs depend on the plane of sectioning (**Figure 3**). For example, circular profiles can be generated by sectioning tubular or spherical structures. *In order to correctly interpret such profiles, microscopists should think in 3D.* In biology, by applying stereological techniques, measurements made on 2D profiles can be extrapolated to their 3D configuration (**Figure 4**).
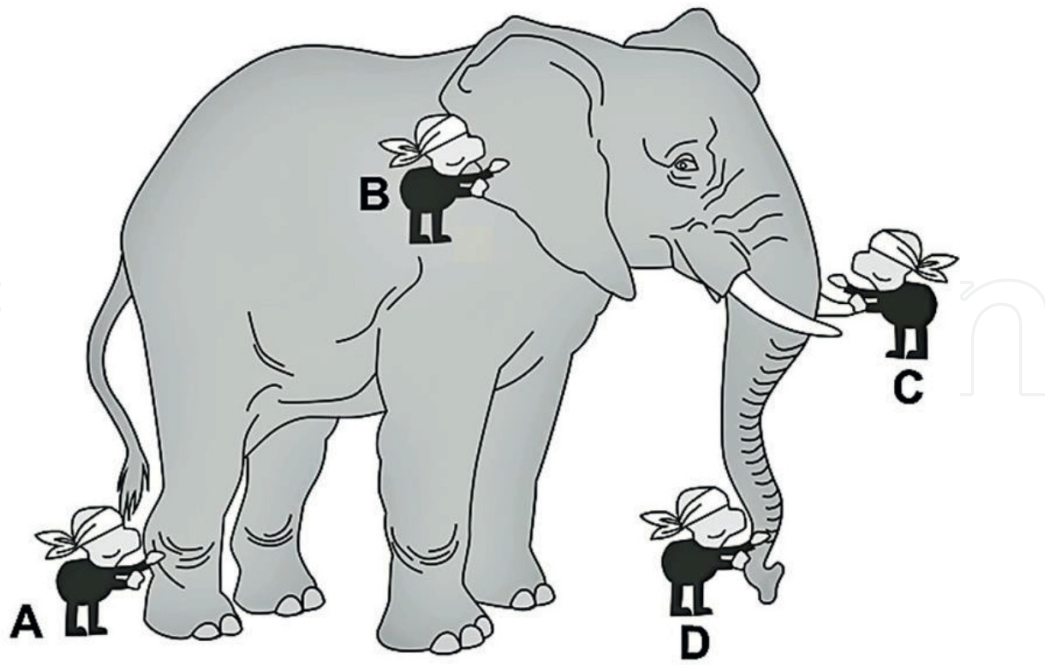
Figure 1. Cartoon showing three blind-folded people palpating different parts of an elephant. The individuals will describe the shape of the elephant differently. Person (A) will, e.g., describe it as corresponding to a trunk of a large tree trunk; (B) will describe it as smooth, flat object; (C) will pronounce it as hard and sharp-pointed; and (D) will deduce it as a soft, pliable object. In principle, all of them are correct. The figure illustrates the following: in quantitative studies, since a whole animal, organ or tissue cannot be analysed piece-by-piece, rigorous sampling has to be undertaken so as to acquire a representative and manageable sample for analysis.
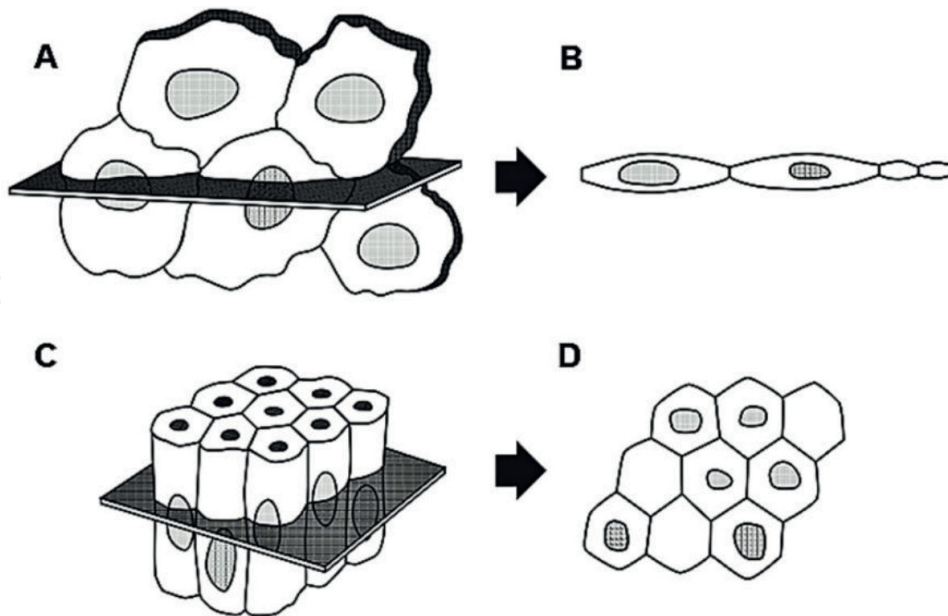

Figure 2. Diagrams showing transversely sectioned epithelial cells (A) and the profiles generated (B) and structures such as muscle fibres (C) that generate profiles when sectioned transversely (D). Stereology allows one to extrapolate measurements made on two-dimensional profiles (B and D) to their three-dimensional configuration.
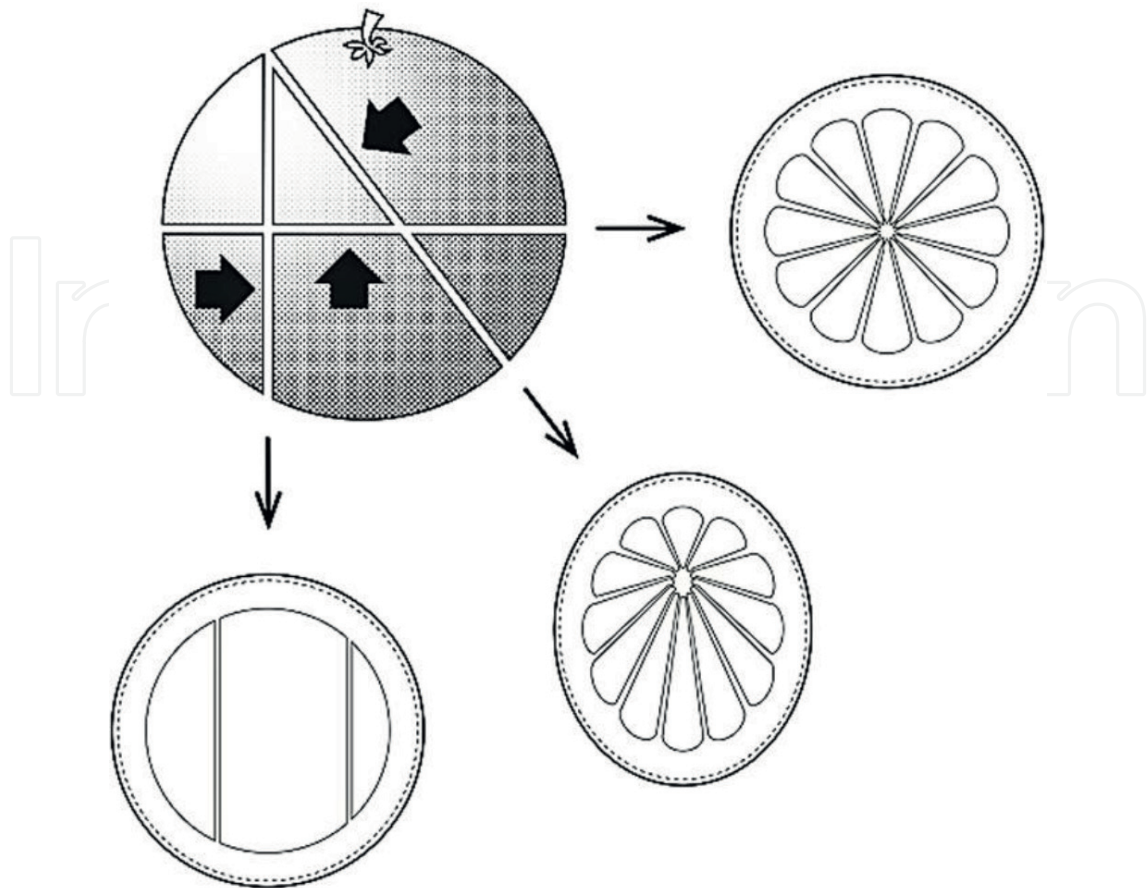
Figure 3. Diagram showing the different profiles that are generated after sectioning a fruit (e.g. an orange) at different planes. By applying stereological methods, the shape of the fruit can be reconstructed from studying sufficient random sections of the fruit.

As a scientific discipline, stereology did not formally start until ∼55 years ago at a meeting of researchers from as varied disciplines as biology, geology, engineering and materials sciences in 1961. A biologist, Professor Hans Elias (specifically a histologist), organized a meeting at Feldberg in Germany which was attended by scientists with one goal in mind: *to quantify 3D images by studying their 2D sections (profiles).* Now called 'The International Society for Stereology and Image Analysis (ISS & IA)', the International Society for Stereology (ISS) was formed at the first congress in Vienna (Austria) in 1962 [4]. Since then, meetings are held regularly, and the ISS is a leading multi-disciplinary collaboration group.

The start of stereology in the 1960s occurred simultaneously with important technological developments that included availability of powerful and affordable microscopes and introduction of innovative tissue preparation and staining techniques such as immunocytochemistry. These developments increased interest in quantitative biology in general and in the emerging field of stereology in particular. Investigators began to prefer the more objective stereological approaches over subjective evaluations that were known to be greatly affected by inter-observer errors. Mathematicians and statisticians in particular have greatly contributed their unique skills to the theoretical aspects of the interdisciplinary discipline of stereology [5]. The major weaknesses in the previous techniques that applied Euclidean formulas based on
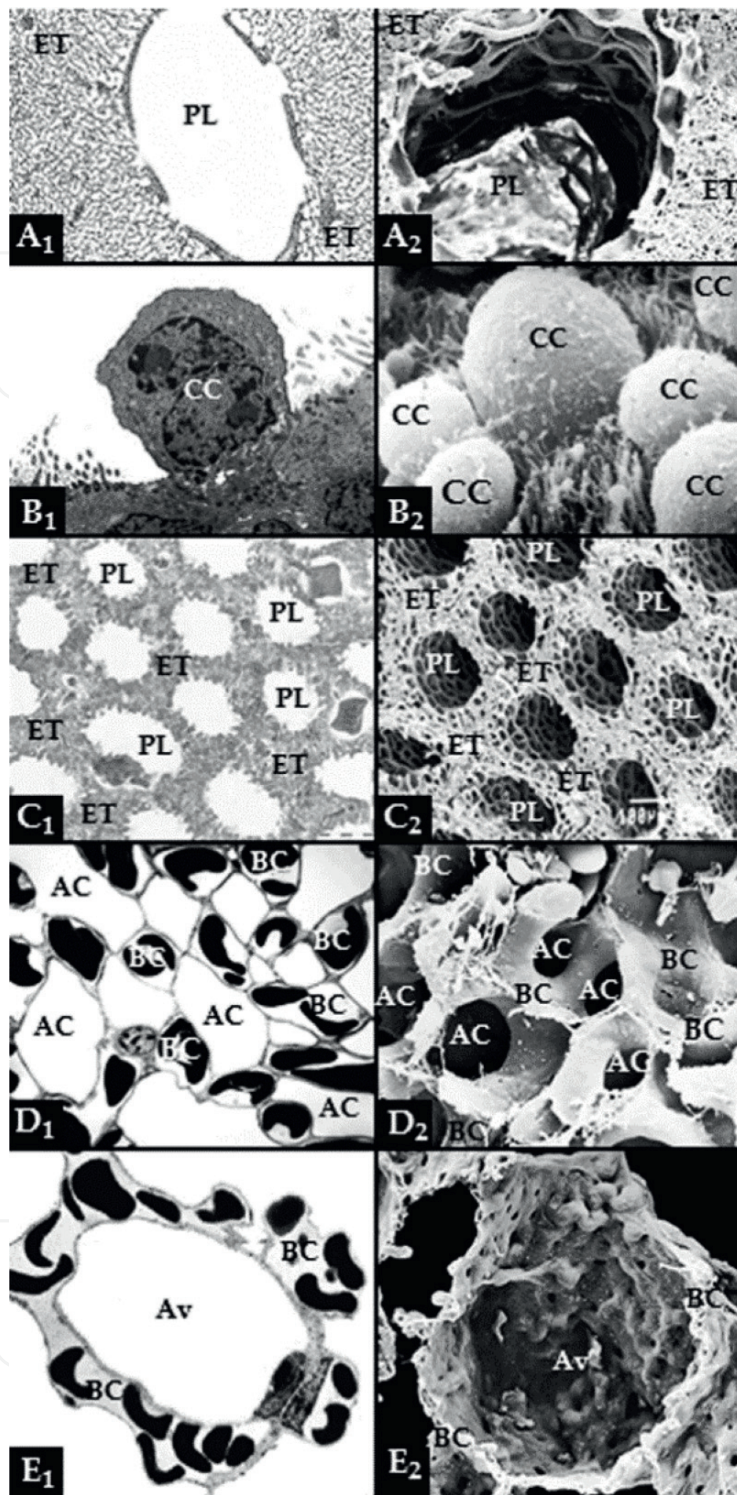
Figure 4. Sectional (2D) images (histological- or transmission electron micrographs) (A_1 to E_1) and corresponding 3D images (scanning electron micrographs) (A_2 to E_2). A_1 and A_2: Parabronchus of the lung of the ostrich, *Struthio camelus* and the domestic fowl, *Gallus gallus* variant domesticus. PL, parabronchial lumen; ET, exchange tissue; B_1 and B_2: Clara cells (CC) of the lung of the greater bush baby, *Galago senegalensis*; C_1 and C_2: Parabronchi of the lung of the domestic fowl. PL, parabronchial lumen; ET, exchange tissue; D_1 and D_2: Structural components of the exchange tissue of the lung of the domestic fowl. AC, air capillaries; BC, blood capillaries and; E_1 and E_2: Alveolus (Av) of the lung from the naked mole rat, *Heterocephalus glaber* and that of the bush baby. BC, blood capillaries. Stereology allows extrapolation of measurements made on 2D profiles (e.g. A_1 to E_1) to their 3D forms (e.g. A_2 to E_2). Absolute parameters such as volume, length, number and surface area can be determined.

classical geometric shapes were identified and improved or replaced with more robust ones. Stereology is a developing science where new innovations continue to make important improvements in the efficiency of the techniques [2, 3]. Utilizing random systematic sampling and different analytical methods, stereology provides unbiased quantitative data.

This account illustrates the versatility of stereological techniques that have contributed greatly to the better understanding of the functional design of the avian lung [6–11]. Many publications, books and programs and algorithms (softwares) are now available on the discipline. Among these are Weibel [2, 5], Stuart [12], Gundersen and Jensen [13], Gundersen and Østerby [14], Mouton [15], Howard and Reed [3] and West [16].

2. The functional design of the avian lung

2.1. Formulation of research question(s)

It is less costly for an animal to fly a given distance per unit time than it is for it to run on the ground across the same distance in the same period of time. This is notwithstanding the fact that powered (active) flight is energetically a very costly form of locomotion [17–19]. The capacity of overcoming gravity and remaining stationary in air (hovering) requires high metabolic capacity and concomitant considerably high consumption of large amounts of O_2 [20, 21]: a hovering hummingbird supports its body weight entirely by power generated by the flight muscles (**Figure 5**). Showing the highly selective nature of flight, powered flight has evolved in only a few animal taxa. It was achieved by insects ~350 million years ago (mya), by the now extinct pterodactyls ~220 mya, birds ~150 mya and bats ~50 mya, chronologically in that order. In terms of speed, endurance and high altitude travel, birds are excellent flyers. For example, a diving peregrine falcon, *Falco peregrinus*, can attain a speed of 403 kph (112 m s^{-1}) [22]; the Arctic tern, *Sterna paradisea*, flies from pole to pole, a return distance of 35,000 km [23, 24]; the American golden plover, *Pluvialis dominica*, flies 3300 km non-stop from the Aleutian Islands to the Hawaiian ones in a time of only 35 h [25]; the wandering albatross (*Diomedea exulans*) of the Southern Oceans flies continuously for days and months without landing [26, 27]; a Ruppell's griffon vulture, *Gyps rueppellii*, was sucked into the engine of a jet-craft at an altitude of 11.3 km [28]; and the bar-headed goose, *Anser indicus*, flies over some of the summits of the Himalayas, altitudes where the barometric pressure is approximately one-third of that at sea level [17, 18, 29].

Among the air-breathing vertebrates, the avian respiratory system, the so-called lung air sac system, is structurally the most complex [8, 30, 31] and functionally the most efficient [32–34].

2.2. Research question

From the above account, the research question posed was: *What are the structural adaptations, specializations and refinements that allow the avian respiratory system to acquire the large amounts of O₂ needed for active and sustained flight under extreme conditions such as high altitude?*
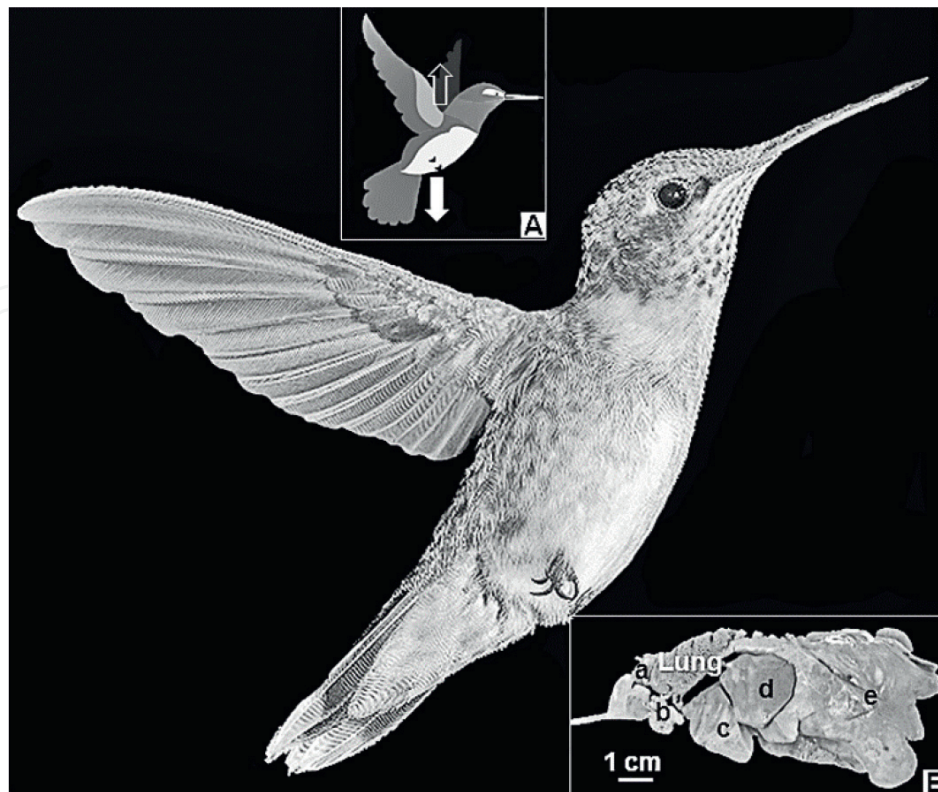
Figure 5. Active (powered) flight in a hummingbird is energetically highly costly. Insert A: In a hovering hummingbird, the body weight (white arrow) is entirely supported by power generated by the flight muscles (open arrow). Insert B. The complex avian respiratory system comprises a lung that is ventilated by air sacs. a: cervical-; b: interclavicular-, c: craniothoracic-; d: caudothoracic, and; e abdominal air sacs.

3. Stereological study of the avian lung

The health of a bird was ascertained before it was killed by sodium pentobarbitone (200 mg cm^{-3}) at a dosage of 0 ± 5 ml kg^{-1} injected into the brachial vein. The body mass was measured for normalization of data to allow intra- and inter-specific comparisons.

3.1. Fixation of the lung

A longitudinal incision was made along the neck and the trachea exteriorized. To avoid cutting any of the blood vessels associated with the neck and inadvertently introducing blood into the respiratory system, the trachea was cannulated through the larynx. The lungs were fixed by intratracheal instillation with 2.5% glutaraldehyde buffered with sodium cacodylate (pH 7.6 and osmolarity 350 mOsm) by gravity at a pressure head of 3000 Pa (1 cm H_2O = 1 mbar = 10^2 Pa). The osmolarity of the fixative was made close to the physiological one of the blood plasma [35] to avoid tissue shrinkage. Osmolarity is a critical factor in morphometric studies because hyperosmotic reagents cause tissue shrinkage, while hypo osmotic ones may cause tissue swelling. Where necessary, shrinkage factors should be determined and introduced in the final calculations. The pressure that was used to fix the lung and the air sacs have been found to be sufficient to drive the fixative into the very narrow terminal respiratory units, the air

capillaries, thereby causing optimal fixation [8]. The fixation of the lung was performed by intratracheal instillation because the method preserves the erythrocytes that are important in the characterization and modelling of the lung: vascular perfusion of the lung washes away the erythrocytes. According to Crapo et al. [36], it also causes relatively greater degree of shrinkage compared to airway instillation. When the fixative stopped flowing down the trachea, the coelomic cavity was gently compressed to expel air trapped in the air sacs and that way increase the penetration of the fixative to different parts of the respiratory system. The trachea was then ligated and the fixative left *in situ* for ~4 h. Thereafter, the lungs were carefully removed from their costovertebral attachments and immersed in fixative.

3.2. Determination of the lung volume

The extrapulmonary primary bronchus was trimmed at the hilum of the lung and the adhering fat and connective tissue removed before the volume of the lung was determined. This was done by weight displacement method [37] (**Figure 6**) which is based on Archimedes' principle that states that a floating body displaces its own weight. Since the specific gravity of the water is unity, the increase in the weight caused by the volume of the fluid displaced by freely
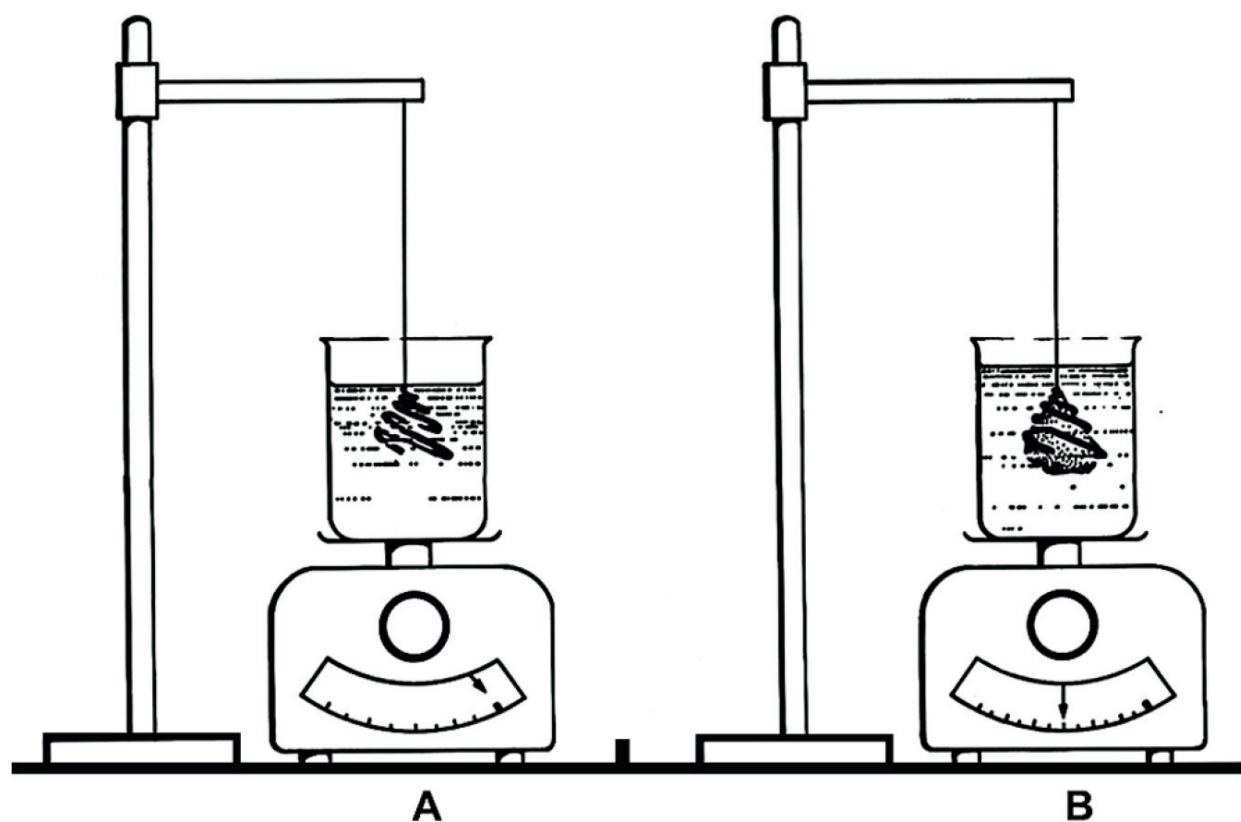

Figure 6. Determination of lung volume by Scherle's method [37] which is based on the Archimede's principle. Because the specific gravity of the lung is less than one and it therefore floats on water, a piece of wire (A) of known volume was used to submerge the lung (B). After the balance was tarred to zero (A) and the lung freely suspended in water (B), the weight increase was equivalent to the volume of the lung because the specific gravity of water is unity.

suspended lung equals its volume. As the specific gravity of the lung is less than one and hence the lung floats to the surface of the water, a metal wire of known volume was used to keep the lung submerged under water. At least three close measurements were made, and the average volume of the lung calculated.

Scherle's [37] method is very accurate in determining volumes of small objects. There being no morphological and morphometric differences between the left and the right avian lungs [8], the left lung was used for light microscopic analyses and the right one for electron microscopy.

3.3. Light microscopic analysis

3.3.1. Tissue processing and sampling

Very small lungs were processed by the standard laboratory techniques, embedded in paraffin wax and serial transverse sections cut craniocaudally at a thickness of 10 μm. The sections were then stained with haematoxylin and eosin. Eight equidistantly spaced, i.e. stratified, sections were taken for analysis. The lungs were cut into slices along the costal sulci and the slices were then cut into halves just dorsal to the primary bronchus (**Figure 7**). Facing cranially, the half slices were processed and embedded in paraffin wax. The first technically adequate section from the cranial face of each half slice was stained with haematoxylin and eosin for analysis.

3.3.2. Determination of volume densities

The volume densities, i.e. the fractional or proportional volumes, of the exchange tissue, the lumina of the parabronchi and secondary bronchi, the blood vessels larger than blood capillaries and the primary bronchus were determined by point-counting at a magnification of 100× using a 100-point Zeiss integrating graticule (**Figure 8**). For example, for the exchange tissue, the volume density ($V_{V(ET)}$) was calculated as follows:

$$V_{V}(ET) = P_{(ET)}.P_{T}^{-1} \tag{1}$$

where $P_{(ET)}$ is the number of points falling onto the exchange tissue and P_{T} the total number of points in the test system or the reference space.

The absolute volumes of the structural components were calculated from the volume of the lung (V_{L}). For example, the absolute volume of the exchange tissue (V_{ET}) was calculated as follows:

$$V_{ET} = V_{V(ET)}.V_{L} \tag{2}$$

The volume densities of the components of the lung that comprise insignificant volume of the lung, e.g. the lymphatics and the inter-parabronchial septa, were not determined. The parabronchi and the secondary bronchi were combined because most of the secondary bronchi have a gas exchange tissue mantle surrounding them, and the small secondary bronchi cannot be well differentiated from the parabronchi.
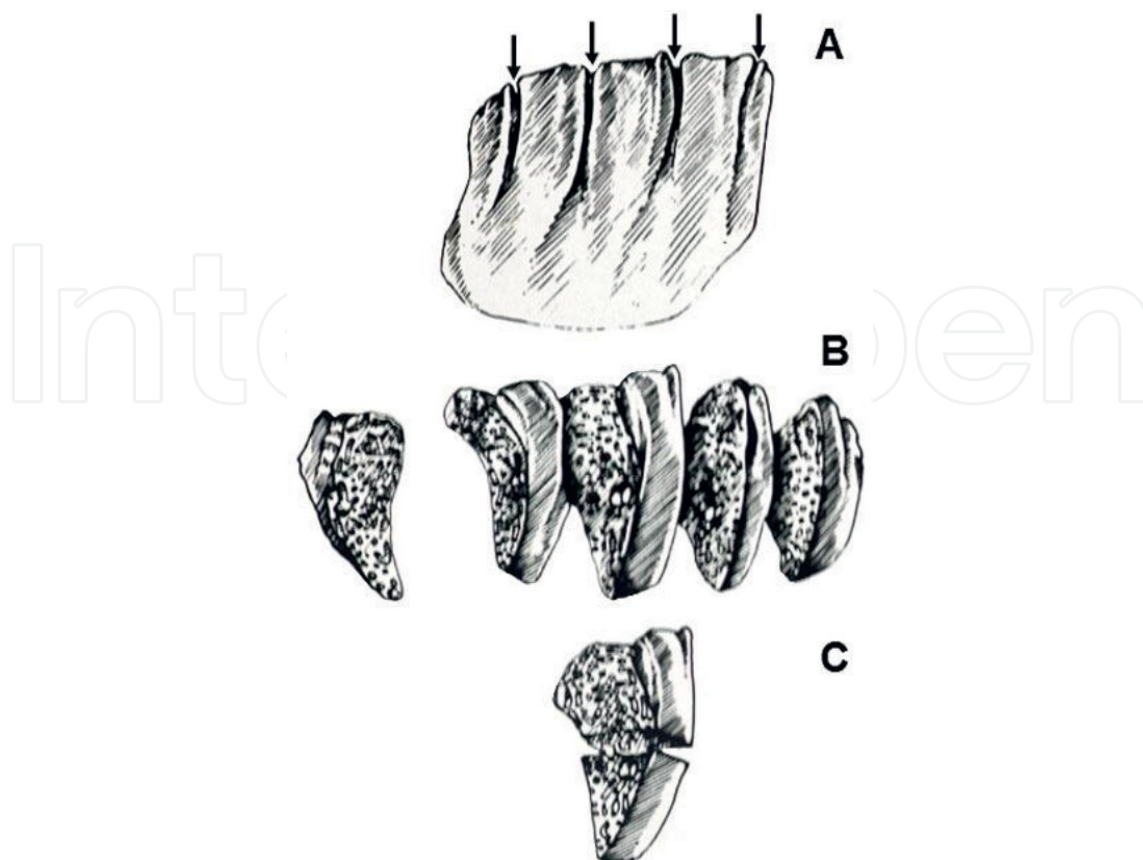
Figure 7. Stratified sampling of the avian lung. The lung (A) was cut into slices along the costal sulci (arrows) (A) and the slices (B) cut into halves just above the primary bronchus (C).

3.3.3. Sample size sufficiency

The adequacy of the number of sections analysed was determined in a pilot study by plotting cumulative average graphs on analysis made on stratified sections, and the sufficiency of the number of points counted for a particular structural component from nomograms given in Weibel [2]. Since the sections were analysed entirely, i.e. field by field, the number of points counted for the three main structural components, i.e. the exchange tissue, the lumina of the parabronchi and the secondary bronchi and the blood vessels larger than blood capillaries, surpassed those needed to give a standard error of the mean of 5% or less.

3.4. Electron microscopic analysis

3.4.1. Tissue processing and sampling

The right lung was cut into slices along the costovertebral sulci and the slices were then cut into halves dorsal to the primary bronchus. The half slices were diced, and the pieces (~1 mm^3 in size) were processed for electron microscopy by the standard laboratory techniques (**Figure 9**). From each half slice, 4–10 blocks were prepared. One block was picked at random and trimmed to remove the rest of the structural components, leaving only the exchange
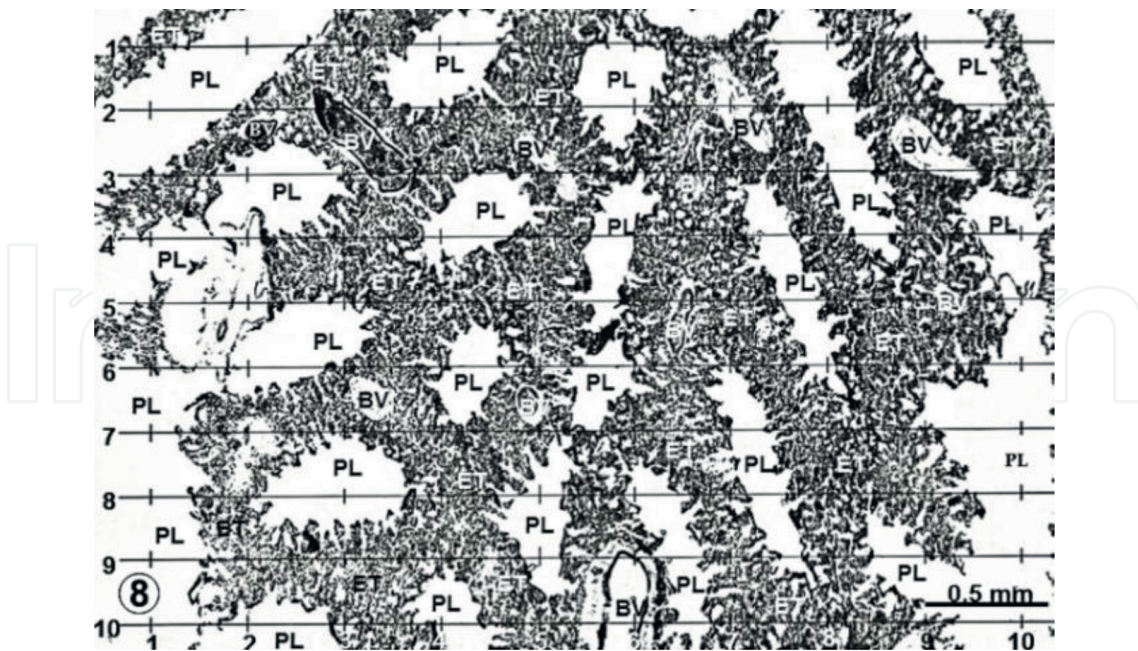
Figure 8. A histological section of the avian lung stained with haematoxylin and eosin. A Zeiss integrating graticule with 100 points was superimposed onto the section. The structural components were analysed by point-counting. PL, parabronchial lumen; ET, exchange tissue; BV, blood vessel larger than blood capillaries.
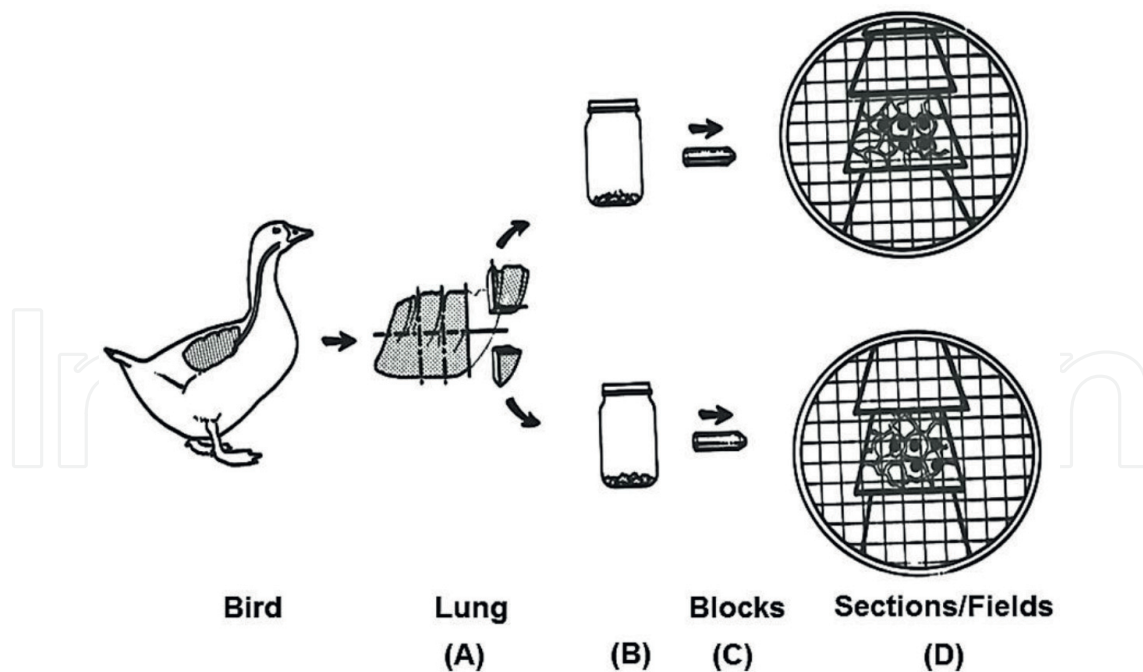

Figure 9. Stratified sampling of the avian lung for transmission electron microscopic analysis. The right lungs were cut transversely along the costal sulci and the slices then cut into halves (A). The halve slices were then diced into small pieces (~1 mm^3) which were embedded in epon (B). From a number of blocks prepared from a half slice, a block (C) was picked at random and ultrathin sections cut and mounted onto 200-wire mesh grids (D). Electron micrographs taken from predetermined areas, i.e., the top right-hand corner of the grid squares (D), to avoid bias.

tissue. Ultrathin sections were cut and mounted on 200-square wire mesh copper grids. Five micrographs were taken from a predetermined corner of the grid squares (the top right corner) to avoid bias at a primary magnification of 3000×. The images were enlarged by a factor of 2.5 and a quadratic lattice grid superimposed on the image (**Figure 10**). On average, for each bird, a total of 40 electron micrographs were analysed at a final magnification of 7500×. In a pilot study, the magnification used for the analysis provided a large field of investigation while providing adequate resolution and permitting the counts and the measurements to be made accurately.

3.4.2. Determination of volume densities

The volume densities of the components of the exchange tissue, namely, the air capillaries, the blood capillaries, the supportive tissue, i.e. the tissue of the blood-gas barrier and the parts of the exchange tissue that are not involved in gas exchange, and the erythrocytes were determined by point counting (**Figure 10**). The intersections of the vertical and the horizontal lines constituted the points used for the determination of the volume densities. For example, the volume density of the air capillaries ($V_{V(ac)}$) was determined as follows:

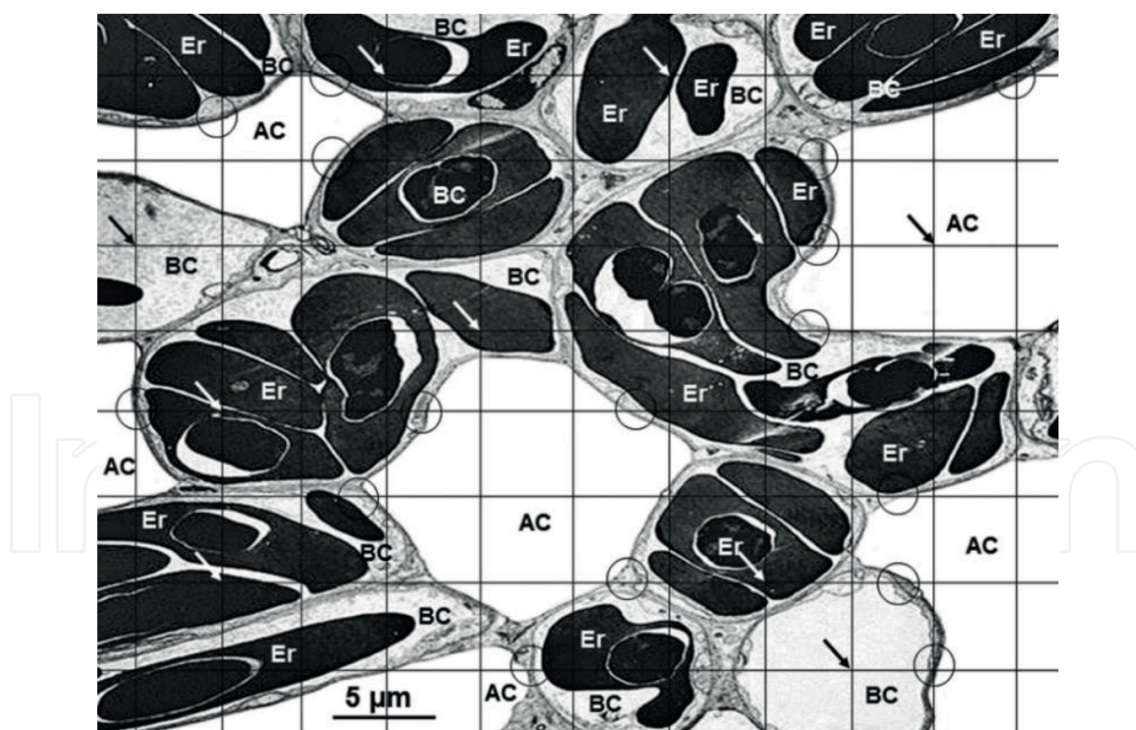$$V_{V}(AC) = P_{(AC)}.P_{T}^{-1} \tag{3}$$

Figure 10. An electron micrograph of the exchange tissue of the avian lung onto which a quadratic lattice grid is superimposed. Points that were formed by the intersections between the vertical and the horizontal lines (arrows) were used to determine the volume densities of the air capillaries (AC), the blood capillaries (BC), the erythrocytes (Er) and the supporting tissue, i.e. the tissue of the blood gas (tissue) barrier and the tissue not involved in gas exchange. The intersections of the horizontal lines with the tissue barriers (circles) were used to determine the surface areas of the air capillaries, the capillary endothelium and the erythrocyte cell membrane.

where $P_{(AC)}$ is the number of points falling onto the air capillaries and P_T the total number of points in the test system.

The absolute volume of the air capillaries (V_{AC}) was calculated from its volume density ($V_{V(AC)}$) and the volume of the exchange tissue (V_{ET}) as follows:

$$V_{(AC)} = V_{V(AC)} . V_{(ET)}^{-1} \qquad (4)$$

3.4.3. Determination of surface densities and surface areas

The surface densities of the blood-gas (tissue) barrier, the blood capillary endothelium and the cell membrane of the erythrocytes were determined by intersection counting, i.e. by counting the crossings of the test system, i.e. the horizontal lines of a quadratic lattice grid, with particular tissue barrier (**Figure 10**). In a pilot study, it had been determined that the number of vertical and horizontal intersections with the barriers were not statistically different. This showed that the
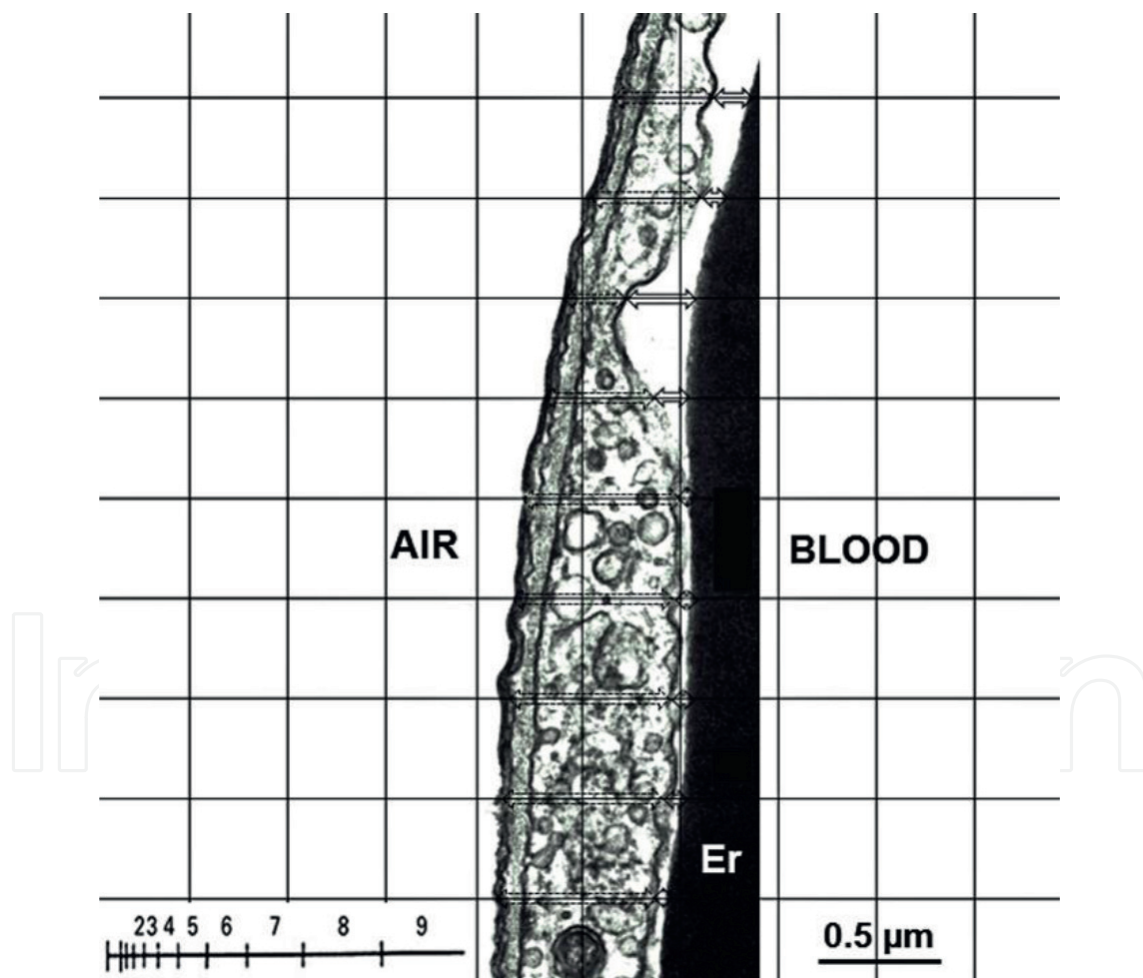
Figure 11. The harmonic thicknesses of the tissue barrier and the plasma layer were determined by intercept length measurement along the horizontal lines of the test grid. The dashed double sided arrows show the intercepts of the blood-gas (tissue) barrier while the continuous double sided ones show those of the plasma layer. A logarithmic scale was used to measure the harmonic mean thickness of the blood-gas (tissue) barrier and the plasma layer. It is shown on the bottom left corner of the figure.

exchange tissue of the avian lung is anisotropic, i.e. homogeneous. For example, the surface density of the blood-gas (tissue) barrier (BGB) ($S_{V(BBG)}$) was calculated as follows:

$$S_{V}(\text{BBG}) = 2I_{Lt} \tag{5}$$

where I is the number of intersections and Lt the total length of the test system in real units, i.e. after correction for the magnification.

The surface area of the blood-gas (tissue) barrier ($S_{A(BGB)}$)was calculated as the product of its surface density (S_V) and the volume of the exchange tissue (V_{ET}) as follows:

$$S_{A}(\text{BGB}) = S_{V(BGB)} . V_{(ET)} \tag{6}$$

3.4.4. Determination of harmonic mean thickness

The harmonic mean thicknesses of the blood-gas (tissue) barrier (τht) and the plasma layer (τhp) were determined from the sum of the reciprocals of the respective intercept lengths (l_h) measured using a logarithmic scale (**Figure 11**). Harmonic mean thickness and NOT arithmetic thickness that weighs the smaller intercepts (thicknesses) compared to the larger ones is the more appropriate estimator of the diffusing capacity, i.e. the conductance, of a barrier to O_2. τht and τhp were calculated as follows:

$$\text{τht} = \tfrac{2}{3} \cdot l_h \tag{7}$$

where l_h is the mean intercept length measured on a logarithmic scale. The mean intercept length was divided by the final magnification to express the thickness in real units.

4. Pulmonary modelling

4.1. General considerations

Following a hierarchy that can be examined on a scale from microscopic to gross, living things are highly organized and structured entities. In larger organisms, cells combine to comprise tissues, which are groups of similar cells performing similar or related functions. Organs are collections of tissues grouped together executing a common function to meaningfully explicate how and why animals work the way they do, biologists must adopt appropriate conceptual models of engineers. On their own, quantitative data do not quite explain the function of an organism or that of its constituent parts. Interestingly, the sum total of the functions performed by the different parts of an organism, e.g. organelles, cells, tissues, organs and organ systems, surpass the function expressed by the whole organism [38, 39]. Hammond et al. [40] stated that 'natural selection operates on organismal-level traits that are usually manifestations of the integrated functioning of a suite of organs and organ systems'. In the complex dynamic biological entities, measurement of physiological changes and processes by testing different structures and measuring separate functions therefore leads to wrong deductions.

Like other organs and organ systems, gas exchangers possess a complex cascading assemblage of structural components that span from cellular- to organ-system level: the structural components are organized as discrete but functionally integrated units. For respiratory organs, the physiological process (gas exchange) that manifests at organismal level is a product of infinitely many small events that are generated by various structural entities at the different levels of organization. Gans [41, 42] pointed out that animals very rarely exhibit one-function-one-structure designs: 'each activity tends to involve multiple aspects of the phenotype and each aspect of the phenotype may be involved in multiple activities'.

Comparative respiratory biologists focus on the structure of gas exchangers and determine how they correlate with properties like function, phylogeny, environment, body size and lifestyle. An insightful study of a gas exchanger or for that matter any other organ should involve application of comprehensive physical models that mathematically integrate the structural and functional aspects of the whole organism/animal.

4.2. Biological models

Scheid [43] remarked that 'models are not only helpful but often indispensable in quantitative biology' and that a model is 'an image of part of the physical or conceptual world apt to explain or predict observations'. Gutman and Bonik [44] termed a model 'an abstraction of a real situation that describes only the essential aspects of the situation'. A mathematical model separates a complex biological structure into its functional parts, sets apart those that are most important in answering particular research questions and then integrates them. A biological model is a mathematical simplification of a complex structure that satisfactorily characterizes the system it describes. It should be simple to apply, easy to understand and theoretically and practically testable.

A simple mechanistic model of a gas exchanger consists of a structure in which the external and the internal respiratory media are separated by a physical (tissue) barrier across which partial pressure gradient of oxygen (PO_2) exists (**Figure 12**). Powell and Scheid [45] pointed out that 'in an attempt at deriving a functional model for gas exchange from morphologic evidence, the physiologist has to identify the simplest functional subunit in the gas exchange organ'. Although biological models are mathematical abstractions of complex systems, since the functions of organs and organisms are regulated by many variables, models should be highly instructive in comparative studies where similar functions are performed by various structures in different ways. To simplify biological models, many structural details have to be omitted and certain assumptions made. The exclusions and the conjectures determine the predictive power of a model. Tweaking a model provides information on the relationship between the physical and functional parameters that drive a biological system. Mathematically adjusting one or more of the parameters and the prevailing conditions under which a system works while holding others constant allows for the identification of constraining, potentiating and redundant factors. The underlying multifaceted control mechanisms that drive the performance of biological components, systems and whole organisms can best be identified by careful modelling.

Figure 12. The main parts of a gas exchanger. Oxygen (O_2) diffuses across a tissue barrier under a partial pressure gradient (large arrow). The conductance of the barrier to O_2 (Dto_2) correlates directly with the surface area (S) and inversely with the thickness of the barrier (t): equation.

4.3. Morphological basis of pulmonary modelling

In accordance with the Fick's law, the conductance or the volume of a gas (e.g. oxygen) that is transferred by diffusion across a tissue barrier per unit time (Do_2) is directly proportional to the surface area (S), the Krogh's permeation coefficient across the tissue barrier (Kto_2) and the partial pressure gradient of O_2 (ΔPo_2). Do_2 correlates inversely with the thickness of the blood-gas (tissue) barrier (t), i.e. the distance O_2 molecules diffuse (**Figure 12**). Fick's law is expressed as follows:

$$Do_2 = Kto_2 \cdot S \cdot \Delta Po_2 \cdot T^{-1} \tag{8}$$

It is the physiologist's equivalent of Ohm's law of electricity which is expressed as follows:

$$I = U \cdot R^{-1} \tag{9}$$

where I is the electric current, U the potential difference (i.e. the voltage) and R the resistance.

The morphometric diffusing capacities of the components of the lung can be estimated from the respiratory surfaces area, the thickness of the air-haemoglobin pathway, the volume of blood in the blood capillaries, the Krogh's O_2 permeation coefficients and the O_2 uptake coefficient of the whole blood [46, 47].

To various extents, the respiratory organs (gas exchangers) have been morphometrically analysed and functionally modelled. These include the fish gills [48] and the lungs of the lungfish (Dipnoi) [49], reptiles [50–53], birds [8, 54–57] and mammals [58–61]. From the concepts and findings of Roughton [62], Roughton and Forster [63], Staub et al. [64] and Sackner et al. [65], a morphometric model was developed by Weibel [66] and later revised in Weibel et al. [67] (**Figure 13**). The relationship between the total pulmonary diffusing capacity of the lung for O_2 (DL_{O_2}) and that of its other parts, namely, the membrane-diffusing capacity (Dm_{O_2}) and the erythrocyte (De_{O_2}) relate as follows:

$$DL_{O_2}{}^{-1} = Dm_{O_2}{}^{-1} + De_{O_2}{}^{-1} \tag{10}$$

De_{O_2} is the product of Θ_{O_2}, the binding rate of O_2 to haemoglobin and the pulmonary capillary blood volume (Vc; Eq. (12)).

Although in all gas exchangers O_2 diffuses across the so-called air-haemoglobin pathway that essentially comprises the blood-gas (tissue) barrier, the plasma layer and to a certain extent, the cytoplasm of the erythrocyte before the molecule is biochemically bound to the haemoglobin, certain modifications of the basic model (**Figures 12** and **13**) have been necessary to satisfy the variations in the morphologies of the different respiratory organs and structures. For example, in birds where the erythrocytes are nucleated, the volume of the pulmonary capillary blood has to be adjusted by 'subtracting' the volume occupied by the nuclei in the erythrocytes [7, 8, 56]. The diffusing capacities of the blood-gas (tissue) barrier (Dt_{O_2}) and the plasma layer (Dp_{O_2}) are estimated from their respective surface areas (S), their harmonic mean thicknesses (τh) and their Krogh's permeation constants (K) for O_2(K_{O_2}). For example, for the blood-gas (tissue) barrier, the diffusing capacity of the barrier (Dt_{O_2}) is calculated as follows:

$$Dt_{O_2} = Kt_{O_2} \cdot St \cdot \tau ht^{-1} \tag{11}$$

where Kt_{O_2} is the Krogh's O_2 permeation constant through the blood-gas (tissue) barrier, St is the surface area of the blood-gas (tissue) barrier and τht is the harmonic mean thickness of the blood-gas (tissue) barrier.

The quantity of blood in the blood capillaries of a respiratory organ determines the amount of O_2 bound by the haemoglobin [63, 68]. The diffusing capacity of the erythrocytes (De_{O_2}) is calculated as follows:

$$De_{O_2} = Vc \cdot \Theta_{O_2} \tag{12}$$

where Vc is the volume of the pulmonary capillary blood and Θ_{O_2} the binding rate of O_2 to haemoglobin. The O_2 permeation constant (K) is a product of the solubility (a) and diffusion (D) constants. Since temperature affects the two factors in opposite directions, i.e. solubility decreases while diffusion increases, Kt_{O_2} is not significantly affected by change in temperature.
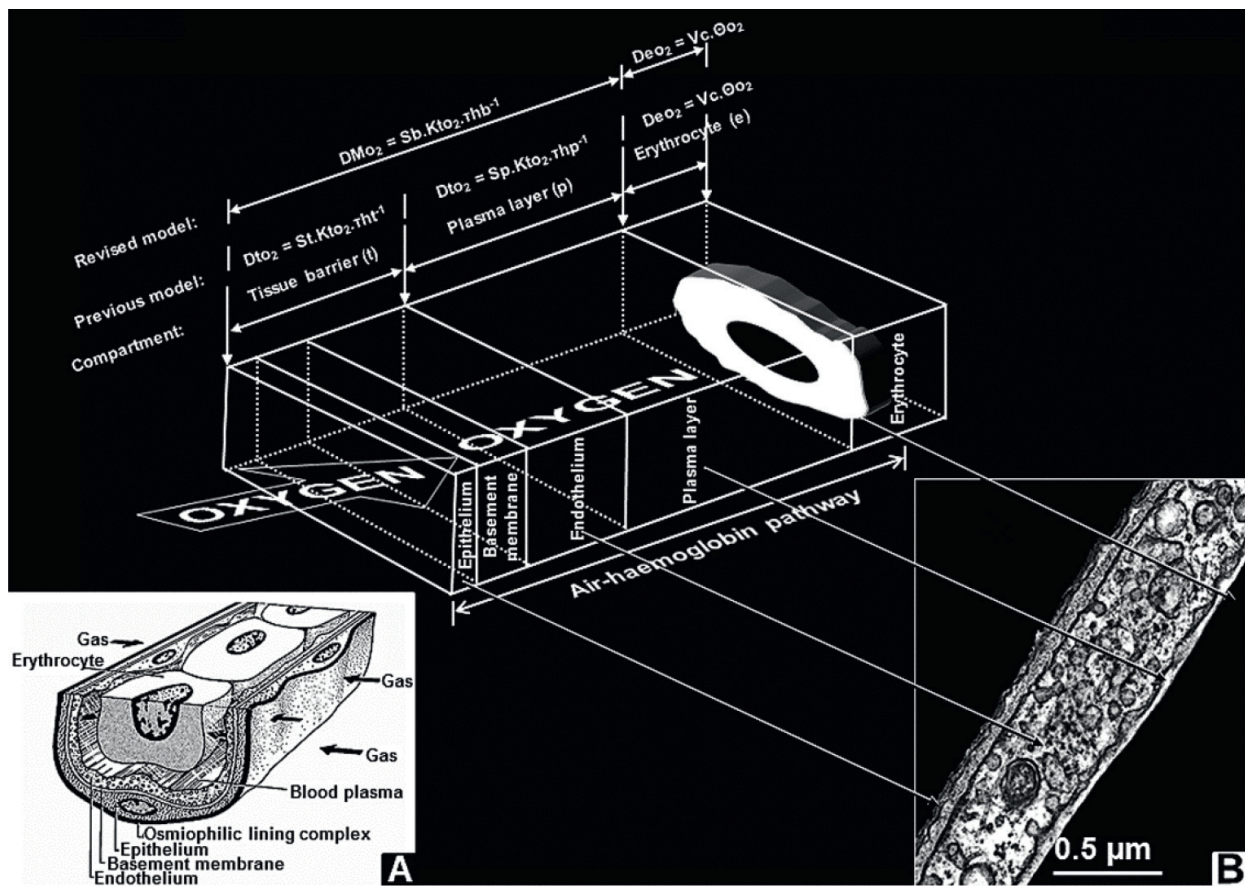
Figure 13. A stereogram showing that in a gas exchanger, oxygen (O_2) diffuses under a partial pressure gradient (large arrow marked oxygen). The barriers through which O_2 diffuses, the so-called the air-haemoglobin pathway, comprises the blood-gas (tissue) barrier, the plasma layer and the cytoplasm of the erythrocyte (RBC). The blood-gas (tissue) barrier consists of an epithelial cell, a basement membrane and an endothelial cell. According to the previous model of Weibel [66], the conductance, i.e., the diffusing capacity of the blood-gas (tissue) barrier for O_2 (Dto_2) is calculated from the surface area of the barrier (St), the O_2 permeation constant through the tissue barrier (Kto_2) and the harmonic mean thickness of the barrier (τht); the conductance of the plasma layer for O_2 (Dpo_2) is calculated from the surface area of the plasma layer (Sp), the O_2 permeation constant through the plasma layer (Kpo_2) and the harmonic mean thickness of the plasma layer (τhp); the conductance of the erythrocyte for O_2 (Deo_2) is calculated from the volume of the pulmonary capillary blood (Vc) and the O_2 uptake coefficient (θo_2). The diffusing capacities correlate directly with the surface areas (S) and the O_2 permeation coefficients (K) and inversely with the thicknesses of the barriers. In the revised model of Weibel et al. [67], the thicknesses of the blood-gas (tissue) barrier and the plasma layers are combined to form the harmonic mean thickness of the total barrier (τhb) and used to calculate the membrane diffusing capacity (Dmo_2). The total (overall) pulmonary morphometric diffusing capacity is calculated from the reciprocals of Dto_2, Dpo_2 [or DMo_2] according to the revised model of Weibel [67] and the Deo_2. Inserts: Insert A: Diagram showing a cross section of a blood capillary which is opened to show erythrocytes and gas (O_2) diffusing through the blood-gas (tissue) barrier and the plasma layer before being bound to the haemoglobin. Insert B: Transmission electron micrograph showing the blood-gas (tissue) barrier and the plasma layer (the air-haemoglobin pathway) of the lung of the domestic fowl, *Gallus gallus* variant *domesticus*.

The barriers that form the air-haemoglobin pathway are arranged in series, i.e. an O_2molecule has to pass through these barriers in succession before it binds to the haemoglobin. Like for electricity when the resistances are arranged in series, in the lung, the total resistance that the molecule encounters can be mathematically expressed as follows:

$$R_L = R_t + R_p + R_e \tag{13}$$

where R_L is the total resistance the lung confers to O_2 molecules and R_t, R_p and R_e are respectively the resistances offered by the blood-gas (tissue) barrier, the plasma layer and the erythrocyte.

According to the 'older' model of Weibel [66], the membrane-diffusing capacity (Dmo_2) is the combined diffusing capacity (conductance) of the blood-gas (tissue) barrier (Dto_2) and the plasma layer (Dpo_2) and is calculated as follows:

$$Dmo_2 = Dto_2 + Dpo_2 \tag{14}$$

In the revised model of Weibel et al. [67], the thickness of the plasma layer is combined with that of the blood-gas (tissue) barrier so that Dmo_2 is calculated as follows:

$$Dmo_2 = S_{(tb)} \cdot \tau hb \tag{15}$$

where $S_{(tb)}$ is the total respiratory surface area and τhb is the harmonic mean thickness of the total barrier, i.e. the distance from the respiratory surface to the cell membrane of the erythrocyte.

The total morphometric pulmonary diffusing capacity (DLo_2) is determined from the diffusing capacities of the blood-gas (tissue) barrier (Dto_2), the plasma layer (Dpo_2) and that of the erythrocytes (Deo_2) as follows:

$$DLo_2 = Dto_2 + Dpo_2 + Deo_2 \tag{16}$$

DLo_2 is an integrative parameter that expresses the structural capacity of the lung to transfer (conduct) oxygen to the body.

4.4. Significance of mathematical modelling in biology

Inexperience and/or unawareness on the technique and lack of physical constants of O_2 permeability through tissues have particularly hindered investigators from mathematically modelling respiratory organs. Comparisons of the functional designs of gas exchangers have largely been based on relating single structural parameters such as lung volumes, respiratory surface areas and thicknesses of the blood-gas barriers. In some cases [50–52], the so-called 'anatomical diffusion factor' (ADF) which is the ratio of respiratory area to the thickness of the blood-gas (tissue) barrier has been used to assess functional efficiencies. Using individual morphometric parameters can lead to wrong conclusions. For example, among birds on which pulmonary morphometric data exist, the Humboldt penguin, *Spheniscus humboldti*, was reported to have a particularly thick blood-gas (tissue) barrier of a harmonic mean thickness of 0.530 μm [57]. If the harmonic mean thickness of the blood-gas (tissue) tissue barrier was used to compare the efficiency of the penguin's lung with those of other birds, it would have been concluded that the gas exchange efficiency of the penguin lung is very poor. However, because like in other diving animals the volume of blood in the lung is very large [69], the total morphometric pulmonary diffusing capacity of the lung of the Humboldt penguin corresponds with those of other species of birds of equivalent body mass [57]. Both in normal and pathological states, changes in the diffusing capacity of the lung can occur anywhere along the air-haemoglobin pathway. In conditions such as pulmonary edema, the thickness of the blood-gas (tissue) barrier increases; in atelectasis

(collapse of the lung), the respiratory surface area decreases; in emphysema, respiratory surface area decreases because of damage of the interalveolar septa; and in some cases of anaemia, the volume of the erythrocytes and therefore the quantity of haemoglobin decreases.

Application of integrative mathematical models on data acquired from biological structures provides robust answers to research questions.

5. Finding

Quantitative analyses of lungs of different species of birds have shown that pulmonary structural refinements correspond with factors such as body mass, lifestyle and habitat occupied [7, 8, 56] (**Figure 14**).
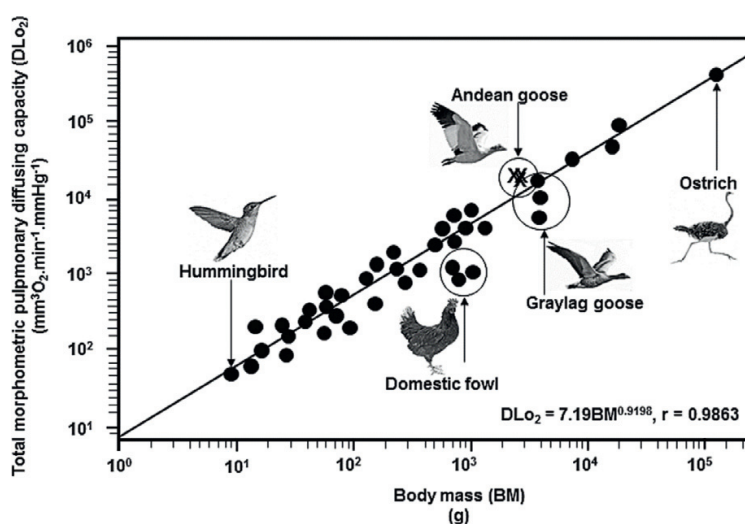

Figure 14. Regression line showing the correlation between the total morphometric pulmonary diffusing capacity (DL_{O_2}) of birds against body mass (BM). Some of the species of birds that have been studied are shown. The data on which the regression line was plotted are given in Maina [7, 8] and Maina et al. [56].

Acknowledgements

Author details

John N. Maina

Address all correspondence to: jmaina@uj.ac.za

Department of Zoology, University of Johannesburg, Johannesburg, South Africa

References

[1] Guex J. Retrograde evolution during major extinction crises. In: Verkhratsky A, editor. Springer Briefs in Evolutionary Biology. Berlin: Springer; 2015. pp. 1–74

[2] Weibel ER. Stereological Methods, Vol. 1: Practical Methods for Biological Morphometry. London: Academic Press; 1979

[3] Howard CV, Reed MG. Unbiased Stereology. 2nd ed. Liverpool: QTP Publications; 2010

[4] Elias H. Address of the president. In: Haug H, editor. Proceedings of the 1st International Congress for Stereology. Wien: Congressprint; 1963. p. 2

[5] Weibel ER. Stereological methods, Vol. 2: Practical Methods for Biological Morphometry. London: Academic Press; 1980

[6] Maina JN. The Gas Exchangers: Structure, Function and Evolution of the Respiratory Processes. Heidelberg: Springer; 1998

[7] Maina JN. The morphometry of the avian lung. In: King AS, McLelland J editors. Form and Function in Birds. Vol. 4. London: Academic Press; 1989; pp. 307–368

[8] Maina JN. The Lung-Air Sac System of Birds: Development, Structure and Function. Heidelberg: Springer; 2005

[9] Maina JN. Development, structure and function of a novel respiratory organ, the lung-air sac system of birds: To go where no other vertebrate has gone. Biological Reviews. 2006;**81**:545–579

[10] Maina JN. The design of the avian respiratory system: Development, morphology and function. Journal of Ornithology. 2015;**156**:41–63

[11] Maina JN, West JB. Thin but strong! The dilemma inherent in the structural design of the blood-water/gas barrier: Comparative functional and evolutionary perspectives. Physiological Reviews. 2005;**85**:811–844

[12] Stuart A. Basic Ideas of Sampling. London: Griffin and Co.; 1984

[13] Gundersen HJG, Jensen EB. The efficiency of systematic sampling in stereology and its prediction. Journal of Microscopy. 1987;**147**:229–262

[14] Gundersen HJG, Østerby R. Optimizing sampling efficiency of stereological studies in biology: Or do more less well. Journal of Microscopy. 1981;**121**:65–73

[15] Mouton PR. Principles of Unbiased Stereology: An Introduction for Bioscientists. Baltimore (MD): John Hopkins University Press; 2002

[16] West MJ. Basic Stereology for Biologists and Neuroscientists. 1st ed. New York: Cold Spring Harbor Laboratory Press; 2012

[17] Bishop CM, Butler PJ. Flight. In: Scanes CG, editor. Sturkie's Avian Physiology. 6th ed. New York: Academic Press; 2015. pp. 919–974

[18] Butler PJ. High fliers: The physiology of bar-headed geese. Comparative Biochemistry and Physiology A. 2010;**156**:325–329

[19] Butler PJ. The physiological basis of bird flight. Philosophical Transactions of the Royal Society B. 2016;**371**:20150384

[20] Bartholomew GA, Lighton JRB. Oxygen consumption during hover-feeding in free-ranging Anna hummingbirds. Journal of Experimental Biology. 1986;**123**:191–199

[21] Wells DJ. Muscle performance in hovering hummingbirds. Journal of Experimental Biology. 1993;**78**:39–57

[22] Tucker VA. Gliding flight: Speed and acceleration of ideal falcons during diving and pull out. Journal of Experimental Biology. 1998;**201**:403–414

[23] Salomonsen F. Migratory movements of the Arctic tern (*Sterna paradisea pontoppidan*) in the Southern Ocean. Det Kongelige Danske Videnskabernes Selskab Biologie Medicine. 1967;**24**:1–37

[24] Egevang C, Stenhouse IJ, Phillips RA, Petersen A, Fox JW, Silk JR. Tracking of Arctic terns, *Sterna paradisea* reveals longest animal migration. Proceedings of the National Academy of Science United State of America. 2010;**107**(5):2078–2081

[25] Johnston DW, McFarlane RW. Migration and bioenergetics of flight in the Pacific golden plover. Condor. 1967;**69**:156–168

[26] Lockley RM. The most aerial bird in the world. Animals. 1970;**13**:4–7

[27] Weimerskirch H, Delord K, Guitteaud A, Phillips RA, Pinet P. Extreme variation in migration strategies between and within wandering albatross populations during their sabbatical year, and their fitness consequences. Scientific Reports. 2015;**5**:8853

[28] Laybourne RC. Collision between a vulture and an aircraft at an altitude of 37,000 ft. Wilson Bulletin. 1974;**86**:461–462

[29] Scott GR, Hawkes LA, Frappell PB, Butler PJ, Bishop CM, Milsom WK. How bar-headed geese fly over the Himalayas. Physiology. 2015;**30**:107–115

[30] King AS. Structural and functional aspects of the avian lung and its air sacs. International Reviews of General Experimental Zoology. 1966;**2**:171–267

[31] Duncker HR. The lung-air sac system of birds. A contribution to the functional anatomy of the respiratory apparatus. Ergebnesse Anatomie Entwicklung. 1971;**45**:1–171

[32] Scheid P. Mechanisms of gas exchange in bird lungs. Reviews of Physiology, Biochemistry and Pharmacology. 1979;**86**:137–186

[33] Fedde MR. The structure and gas flow pattern in the avian lung. Poultry Science. 1980;**59**:2642–2653

[34] Powell FL. Respiration. In: Scanes C, editor. Sturkie's Avian Physiology. 6th ed. San Diego: Elsevier; 2015. pp. 301–336

[35] Sykes AH. Formation and composition of urine. In: Bell DJ, Freeman BM, editors. Physiology and Biochemistry of the Domestic Fowl. London: Academic Press; 1971. pp. 233–278

[36] Crapo JD, Crapo RO, Jensen RL, Mercer RR, Weibel ER. Evaluation of lung diffusing capacity by physiological and morphometric techniques. Journal of Applied Physiology. 1988;**64**:2083–2091

[37] Scherle WF. A simple method for volumetry of organs in quantitative stereology. Mikroskopie. 1970;**26**:57–60

[38] Thompson D'AW. On Growth and Form. 2nd ed. Cambridge: Cambridge University Press; 1959

[39] Hoagland M, Dodson B. The Way Life Works. London: Ebury Press; 1995

[40] Hammond KA, Chappell MA, Cardullo RA, Lin RS, Johnsen TS. The mechanistic basis of aerobic performance variation in red jungle fowl. Journal of Experimental Biology. 2000;**203**:2053–2064

[41] Gans C. Vertebrate morphology: Tale of a phoenix. American Zoologist. 1985;**25**:689–694

[42] Gans C. Adaptation and the form-function relation. American Zoologist. 1988;**28**:681–697

[43] Scheid P. The use of models in physiological studies. In: Feder ME, Bennett AF, Burggrenn WW, Huey RB, editors. New Direction in Ecological Physiology. Cambridge: Cambridge University Press; 1987. pp. 275–288

[44] Gutman WF, Bonik K. Kritische Evolutionstheorie. Gerstenberg: Hildesheim; 1981

[45] Powell FL, Scheid P. Physiology of gas exchange in the avian respiratory system. In: King AS, McLelland J, editors. Form and Function of the Avian Lung. Vol. 4. London: Academic Press; 1989. pp. 393–437

[46] Vandergriff KD, Olson JS. Morphological and physiological factors affecting oxygen uptake and release by red blood cells. Journal of Biological Chemistry. 1984;**259**:12619–2627

[47] Yamaguchi K, Nguyen-Phu D, Scheid P, Piiper J. Kinetics of oxygen uptake and release by human erythrocytes studied by a stopped-flow technique. Journal of Applied Physiology. 1985;**58**:215–1224

[48] Hughes GM. Morphometrics of the fish gills. Respiration Physiology. 1972;**14**:1–25

[49] Hughes GM, Weibel ER. Morphometry of fish lungs. In: Hughes GM, editor. Respiration of Amphibious Vertebrates. London: Academic Press; 1976. pp. 213–232

[50] Perry SF. Quantitative anatomy of the lungs of the red-eared turtle, *Pseudemys scripta elegans*. Respiration Physiology. 1978;**35**:245–262

[51] Perry SF. Morphometric analysis of pulmonary structure: Methods for evaluation and comparison of unicameral lungs. Microskopie. 1981;**38**:278–293

[52] Perry SF. Reptilian lungs: Functional anatomy and evolution. Advances in Anatomy Embryology and Cell Biology. 1983;**79**:1–81

[53] Perry SF. Recent advances and trends in the comparative morphometry of vertebrate gas exchange organs. In: Boutilier RG, editor. Advances in Comparative and Environmental Physiology. Heidelberg: Springer-Verlag; 1990. pp. 45–71

[54] Maina JN. Functional morphology of the avian respiratory system, the lung-air sac system: Efficiency built on complexity. Ostrich. 2008;**79**:117–132

[55] Maina JN. Morphometrics of the avian lung: The structural-functional correlations in the design of the lungs of birds. Comparative Biochemistry and Physiology. 1993;**105A**:397–410

[56] Maina JN, King AS, Settle G. An allometric study of the pulmonary morphometric parameters in birds, with mammalian comparison. Philosophical Transactions of the Royal Society of London. 1989;**326B**:1–57

[57] Maina JN, King AS. A morphometric study of the lung of the Humboldti penguin *(Spheniscus humboldti)*. Zentralbrat Veterinary Medicine C, Anatomy, Histology and Embryology. 1987;**16**:293–297

[58] Weibel ER. The Pathways for Oxygen: Structure and Function in the Mammalian Respiratory System. Harvard: Harvard University Press (Mass); 1984

[59] Weibel ER. Lung morphometry and models in respiratory physiology. In: Chang HK, Paiva M, editors. New York: Marcel Dekker; 1989. pp. 1–56

[60] Weibel ER. Morphometry: Stereological theory and practical methods. In: Gill J, editor. Models of Lung Disease: Microscopy and Structural Methods. New York: Marcel Dekker; 1990. pp. 199–251

[61] Gehr P, Mwangi DK, Ammann A, Maloiy GMO, Taylor CR, Weibel ER. Design of the mammalian respiratory system: V. Scaling morphometric diffusing capacity to body mass: Wild and domestic animals. Respiration Physiology. 1981;**44**:61–86

[62] Roughton FJW. The average time spent by the blood in the human lung capillary and its relation to the rate of CO_2 uptake and elimination. American Journal of Physiology. 1945;**14**:3621

[63] Roughton FJW, Forster RE. Relative importance of diffusion and chemical reaction rates in determining rate of O_2 exchange of pulmonary membrane and volume of blood in lung capillaries. Journal of Applied Physiology. 1957;**11**:290–302

[64] Staub NG, Bishop JM, Forster RE. Importance of diffusion and chemical reaction rates in oxygen uptake in the lung. Journal of Applied Physiology. 1962;**17**:21–27

[65] Sackner MA, Greeneltch D, Heiman MS, Epstein, LS, Atkins N. Diffusing capacity, membrane diffusing capacity, capillary blood volume, pulmonary tissue and cardiac output measured by a rebreathing technique. American Review of Respiratory Diseases. 1975;**111**:157–165

[66] Weibel ER. Morphometric estimation of pulmonary diffusion capacity. I. Model and method. Respiration Physiology. 1970/71;**11**:54–75

[67] Weibel ER, Federspiel WJ, Fryder-Doffey F, Hisia CCW, Konnig M, Stalder-Navarro V, Vock R. Morphometric model for pulmonary membrane diffusing capacity. Respiration Physiology.1993;**93**:125–149

[68] Cotes JE. Lung Function: Assessment and Application in Medicine. 2nd ed. Oxford: Blackwell Scientific; 1968

[69] Andersen HT. Physiological adaptations in diving vertebrates. Physiological Reviews 1966;**46**:212–243